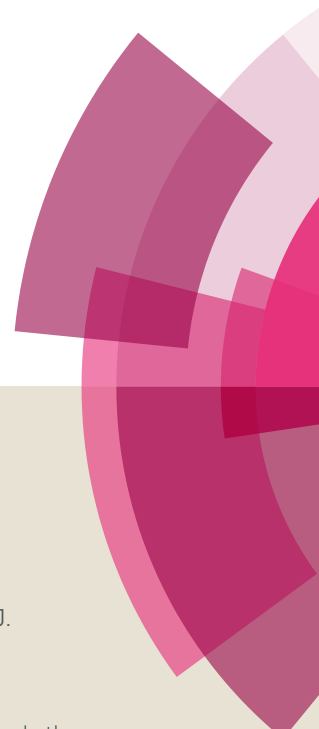
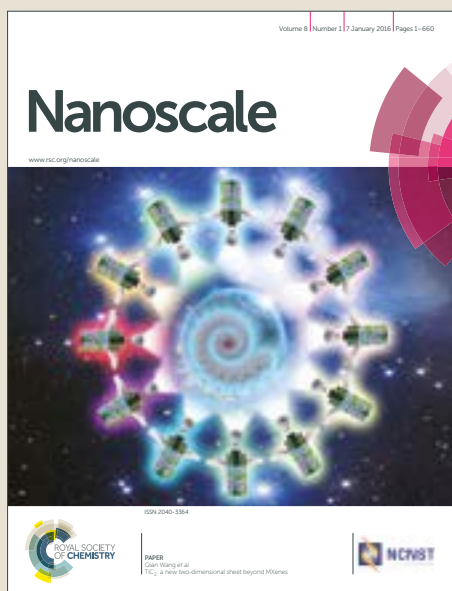


# Nanoscale

Accepted Manuscript



This article can be cited before page numbers have been issued, to do this please use: A. Bezryadina, J. Li, J. Zhao, A. Kothambawala, J. L. Ponsetto, E. Huang, J. Wang and Z. Liu, *Nanoscale*, 2017, DOI: 10.1039/C7NR03654J.



This is an Accepted Manuscript, which has been through the Royal Society of Chemistry peer review process and has been accepted for publication.

Accepted Manuscripts are published online shortly after acceptance, before technical editing, formatting and proof reading. Using this free service, authors can make their results available to the community, in citable form, before we publish the edited article. We will replace this Accepted Manuscript with the edited and formatted Advance Article as soon as it is available.

You can find more information about Accepted Manuscripts in the [author guidelines](#).

Please note that technical editing may introduce minor changes to the text and/or graphics, which may alter content. The journal's standard [Terms & Conditions](#) and the ethical guidelines, outlined in our [author and reviewer resource centre](#), still apply. In no event shall the Royal Society of Chemistry be held responsible for any errors or omissions in this Accepted Manuscript or any consequences arising from the use of any information it contains.

## Localized plasmonic structured illumination microscopy with optically trapped microlens

Anna Bezryadina,<sup>a</sup> Jinxing Li<sup>b</sup>, Junxiang Zhao<sup>a</sup>, Alefia Kothambawala<sup>a</sup>, Joseph Ponsetto<sup>a</sup>, Eric Huang<sup>c</sup>, Joseph Wang<sup>b</sup>, Zhaowei Liu<sup>\*a</sup>

Received 23th May 2017,  
Accepted 00th January 20xx

DOI: 10.1039/x0xx00000x

[www.rsc.org/nanoscale](http://www.rsc.org/nanoscale)

Localized plasmonic structured illumination microscopy (LPSIM) is a recently developed super resolution technique that demonstrates immense potential via arrays of localized plasmonic antennas. Microlens microscopy represents another distinct approach for improving resolution by introducing spherical lens with large refractive index to boost the effective numerical aperture of the imaging system. In this Paper, we bridge together the LPSIM and optically trapped spherical microlenses, for the first time, to demonstrate a new super resolution technique for surface imaging. By trapping and moving polystyrene and TiO<sub>2</sub> microspheres with optical tweezers on top of a LPSIM substrate, the new imaging system has achieved higher NA and resolution improvement.

### Introduction

The development of the optical microscope revolutionized life and material science; however, the resolution of conventional microscopes is limited to the half-wavelength scale (200–300nm) due to the diffractive nature of the illuminating light. In modern medicine and biology there is a strong demand for surface imaging of various objects and processes at size scales far below the diffraction limit of visible light. Recent super resolution microscopy techniques, such as stimulated emission depletion microscopy (STED)<sup>1–3</sup>, stochastic optical reconstruction microscopy (STORM)<sup>4,5</sup>, and photoactivated localization microscopy (PALM)<sup>6</sup> have been demonstrated and attracted much attentions. These methods have greatly improved the spatial resolution to sub-50nm scales in all three dimensions, but also significantly sacrificed other imaging capabilities such as imaging speed, field of view, simplicity of the system, as well as photo toxicity. Structured illumination microscopy (SIM)<sup>7–11</sup> can achieve reasonable speed and wide field of view simultaneously, but its resolution is limited to ~2 times better than the diffraction limit, i.e. about 84nm when in combination with total internal reflection fluorescence (TIRF) and the best available ultrahigh NA objective<sup>12</sup>.

Recently, plasmonics has been introduced to the field of SIM to further improve its resolution. For instance, plasmonic structure illumination microscopy (PSIM) utilizes the surface

plasmon interference to replace the traditional projected light pattern, so that the resolution improvement can surpass 2 times that of the diffraction limit<sup>13–16</sup>. Localized plasmon structured illumination microscopy (LPSIM) employs near-field excitation from the localized surface plasmons of fine periodic structures<sup>17,18</sup>. With this unique super resolution technique and 1.2NA objective, wide-field surface imaging with resolution down to 75 nm was demonstrated. This represents ~3 times resolution improvement compared with conventional epi-fluorescence microscopy, while maintaining reasonable speed and compatibility with biological specimens<sup>18</sup>. Both PSIM and LPSIM also rely on the spatial frequency mixing between the illumination patterns and the object, therefore the super resolution image must be numerically reconstructed using a SIM<sup>19</sup> or blind SIM reconstruction method<sup>14,18,20</sup>. The resonant plasmonic enhancement of the localized plasmonic fields provides strong excitation of targeted fluorescent labels, which allows shorter exposure times thus faster imaging speeds.

Currently, all SIM technologies are using commercial objectives for image collection, so that the objective NA becomes a major limiting factor. Combining dielectric microspheres with low NA objectives has been proven as a valuable scheme to improve the effective NA of the imaging system for resolving much finer structures<sup>21–28</sup>. By placing high-index dielectric microspheres close to the investigation surface, near-field coupling occurs and an extraordinary sharp focus (so-called “photonic nanojet”) with local strongly enhanced imaging has been demonstrated<sup>23,24,27</sup>. Although the mechanisms for this enhanced resolution has been debated in literatures<sup>22–25,28</sup>, it is commonly believed that the high refractive index of the microlenses increases the total effective NA of the imaging system, leading to the improved resolution. For practical applications, the microlenses typically need to be

<sup>a</sup> Department of Electrical and Computer Engineering, University of California, San Diego, La Jolla, California 92093, USA. E-mail: zhaowei@ucsd.edu

<sup>b</sup> Department of Nanoengineering, University of California, San Diego, La Jolla, California 92093, USA.

<sup>c</sup> Department of Physics, University of California, San Diego, La Jolla, California 92093, USA.

Electronic Supplementary Information (ESI) available. See DOI: 10.1039/x0xx00000x

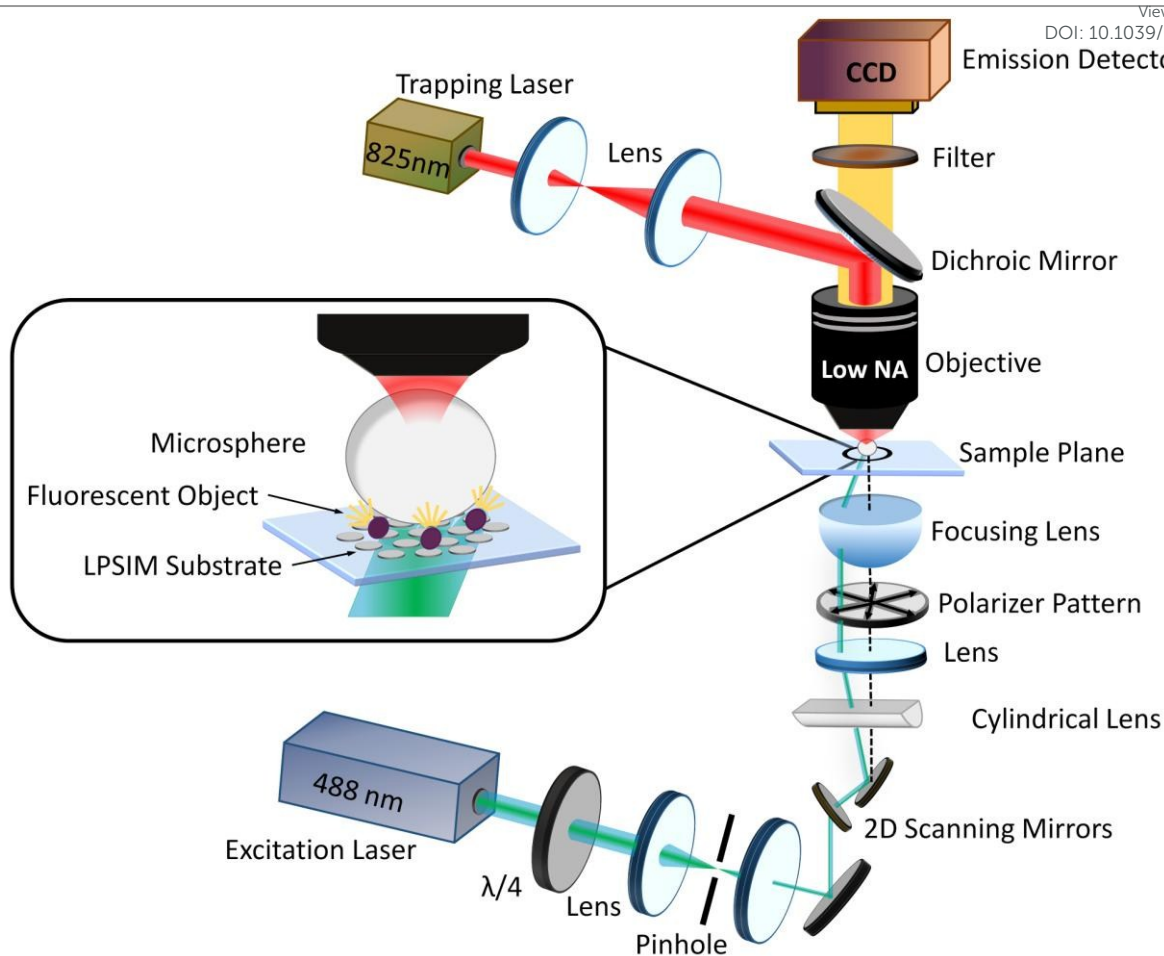


**Fig. 1** Schematic diagram of OT-LPSIM experimental setup. An excitation laser is directed via 2D scanning mirrors through a 4f system which defines the angle of laser incidence to the LPSIM substrate. In-plane polarization regardless of angle is guaranteed by a custom-made polarizer plate, which ensures the correct excitation patterns. An IR trapping laser is used to move and control the position of the microlens, then the objective, filtered, and passed to the emission detector CCD.

mobile to reach the desired location, which can be guided by fine glass micropipettes<sup>29</sup>, optical tweezers<sup>30-37</sup>, electrostatic attachment to AFM tip<sup>38</sup> or chemical propulsion<sup>39</sup>. In this paper, by combining near-field microlens with LPSIM for the first time, we report a new microscopy technique which offers advantages over existing super-resolution imaging methods with significantly improved resolution.

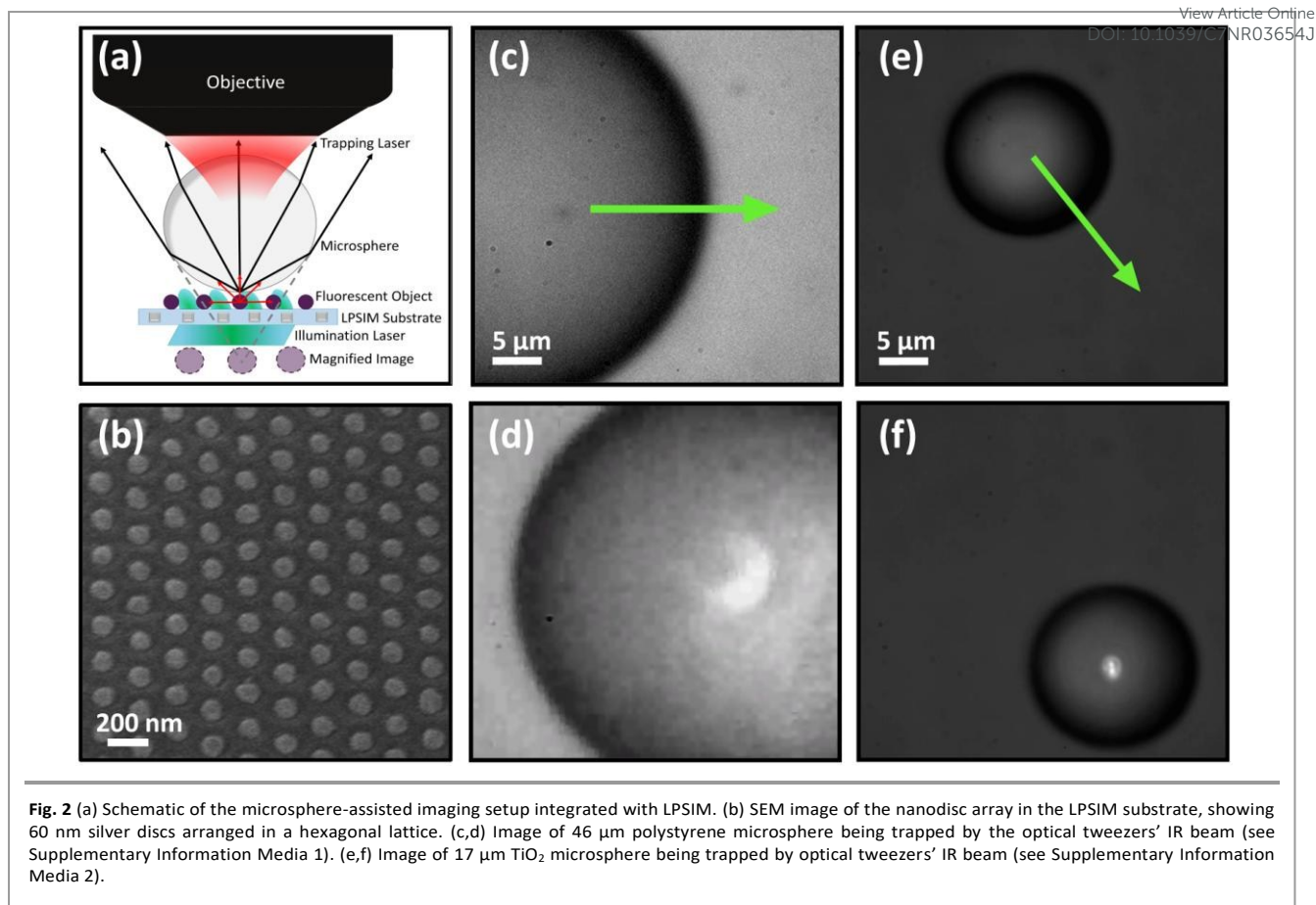
## Experimental

### Experimental set-up

The schematic diagram of the new microscopy system, i.e. optical tweezers based LPSIM (OT-LPSIM), is shown in Figure 1. For the LPSIM illumination part of the system, the excitation laser beam passes through two galvanometer scanning mirrors, a lens and microscope objective in a 4f system, and then illuminates the plasmonic substrate, creating the plasmonic structured illumination excitation pattern. The beam polarization and illumination angle incident to the plasmonic structure was controlled by radially orientated polarizer strips (in front of the objective) and the galvo

scanners, respectively. The fluorescent emission excited by the plasmonic structure was collected by the microsphere and an objective, and form diffraction-limited images at the CCD camera (see Figure 2a). The trapped microsphere acts like a movable microlens and allow the user to interactively zoom into the field of interest together with the objective. For the optical trapping and manipulation of the microsphere we use a continuous wave 825 nm laser (20-30mW), which is compatible for future biological applications and has low optical damage<sup>31,40</sup>. The collimated expanded infrared (IR) laser was emitted from the top and focused in the observation plane by the same imaging objective.

The LPSIM substrates we used include a hexagon lattice array of 60 nm silver discs with a 150 nm pitch embedded in silica, as shown in Figure 2b. When polarized laser light hits the plasmonic nano-discs array, it creates evanescent fields which illuminate fluorescent objects in the near field<sup>18</sup>. By optically trapping microsphere lens on top of LPSIM substrate with fluorescent objects, the LPSIM sub-images are further magnified and collected by a much higher effective NA of the system, leading to greatly improved LPSIM resolution while using relatively low NA objective.



### Optically controlled microspheres

By altering the sizes and materials of microspheres immersed in varied liquids, we could achieve different effective NA, resolutions, and magnifications below a sphere<sup>25</sup>. The image magnification of the sphere, can be roughly approximated by geometric optics  $M = n_r / (2 - n_r)$ , where  $n_r$  is a relative index contrast of microsphere and surrounding medium<sup>22</sup>. For the best of imaging quality, the optimal relative index contrast  $n_r$  between microsphere and media is 1.4-1.75<sup>22,23</sup>. The polystyrene spheres (the index of refraction  $n = 1.59$ ) in water ( $n = 1.33$ ) have low relative index contrast 1.2, but they are commercially available in vast range of sizes and can be easily optically trapped<sup>34,36</sup>. The TiO<sub>2</sub> spheres ( $n = 2.1$ ) in water have optimal relative index contrast 1.58 for imaging, but according to the theoretical predictions the particle trapping efficiency could strongly depend on the sphere size<sup>34</sup>. The theoretical magnifications for polystyrene and TiO<sub>2</sub> spheres are 1.48 and 3.76, respectively. Since spheres are micro-sized, for the same material the real experimental magnification non-linearly varies on sphere's radius<sup>24,25</sup>. Also to move a microsphere with optical tweezers without disturbing sample, we need to have a tiny gap between the microsphere and the LPSIM substrate, which also could slightly affect the magnification<sup>41</sup>. So for different sphere sizes, the magnification properties can vary and should be estimated experimentally.

For our experiment, we primarily used two types of microspheres: ~45 μm diameter polystyrene spheres with 1.55 magnification and ~20 μm TiO<sub>2</sub> spheres with 3.6 magnification, both of which are optically trapped in water and free to be moved to the desired area. The exact magnification for each sphere was estimated by measuring distances between fluorescent beads with and without sphere in front of them. In Figure 2c-f and Supplementary Information Media 1 and Media 2 we demonstrate the trapping and movement of both types of spheres with optical tweezers. Larger spheres were later used to maximize the magnified area below the sphere and to demonstrate the performance of OT-LPSIM. In general, 30% of the area below the center of the sphere can be safely used for reconstruction without much aberration.

## Results and discussion

### Polystyrene microspheres

To test the super-resolution imaging performance of our OT-LPSIM system, 40 nm fluorescent beads (570 nm emission) were drop-casted and fixed onto the LPSIM substrate, and were imaged through a 46 μm polystyrene microsphere. The polystyrene sphere can be trapped and moved into the area of interest (Figure 3a-c) at significantly lower laser power, since the sphere was not only trapped by the direct laser beam from the objective but also by the reflected beam from the

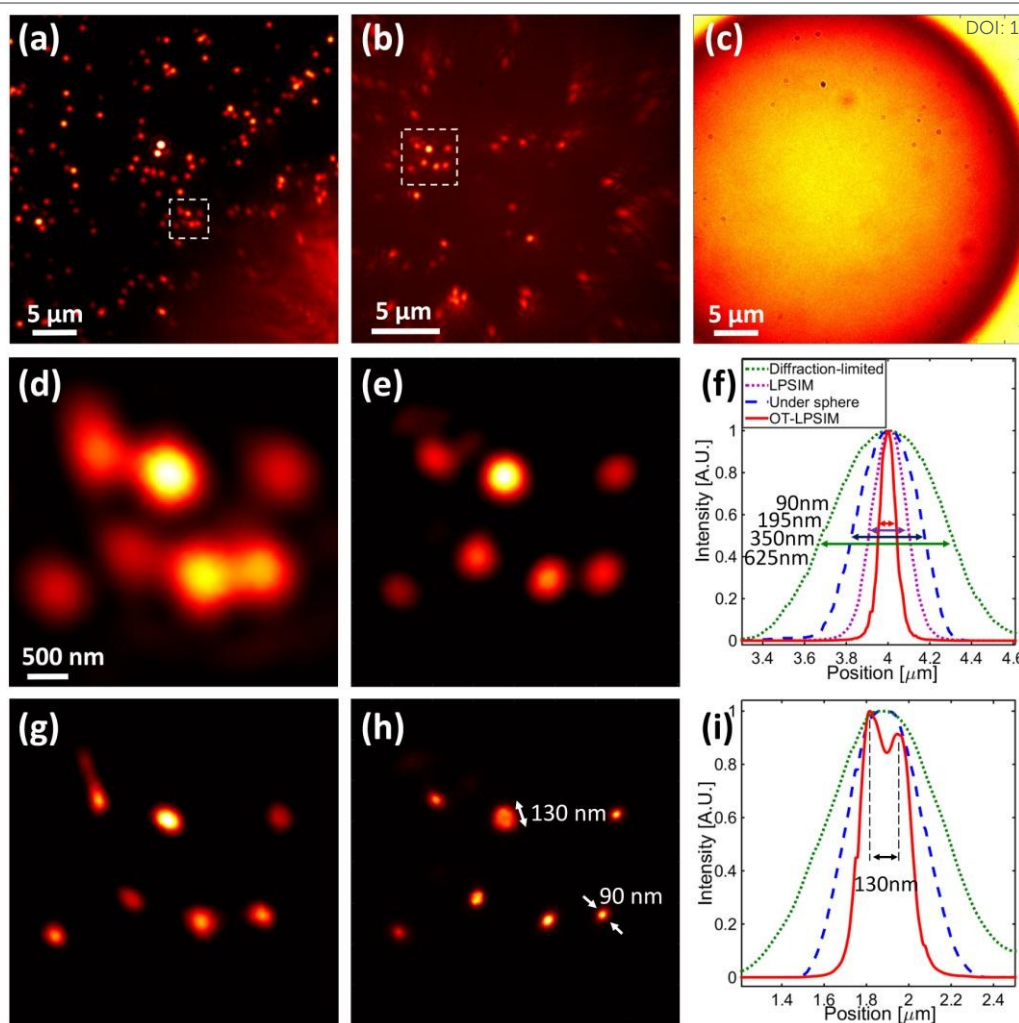


**Fig. 3** (a) Fluorescence image of 40 nm beads through a 60X (0.8NA) objective lens under 488 nm excitation. (b) Fluorescent beads are magnified 1.55 times under polystyrene microsphere. The microscope objective was focused on the virtual images formed underneath the sphere. (c) Image of 46  $\mu\text{m}$  diameter movable polystyrene sphere. (d) Diffraction-limited image of the selected area in (a). (e) Corresponding magnified image of (b) under microlens with significantly improved resolution. (g) LPSIM reconstructed image of (d). (h) OT-LPSIM reconstructed image of (e). (f,i) Quantification of the experimental resolution in (d,e,g,h) using the intensity profile. Standard FWHM: 625 nm; FWHM with microlens: 350 nm; LPSIM FWHM: 195 nm; OT-LPSIM FWHM: 90 nm.

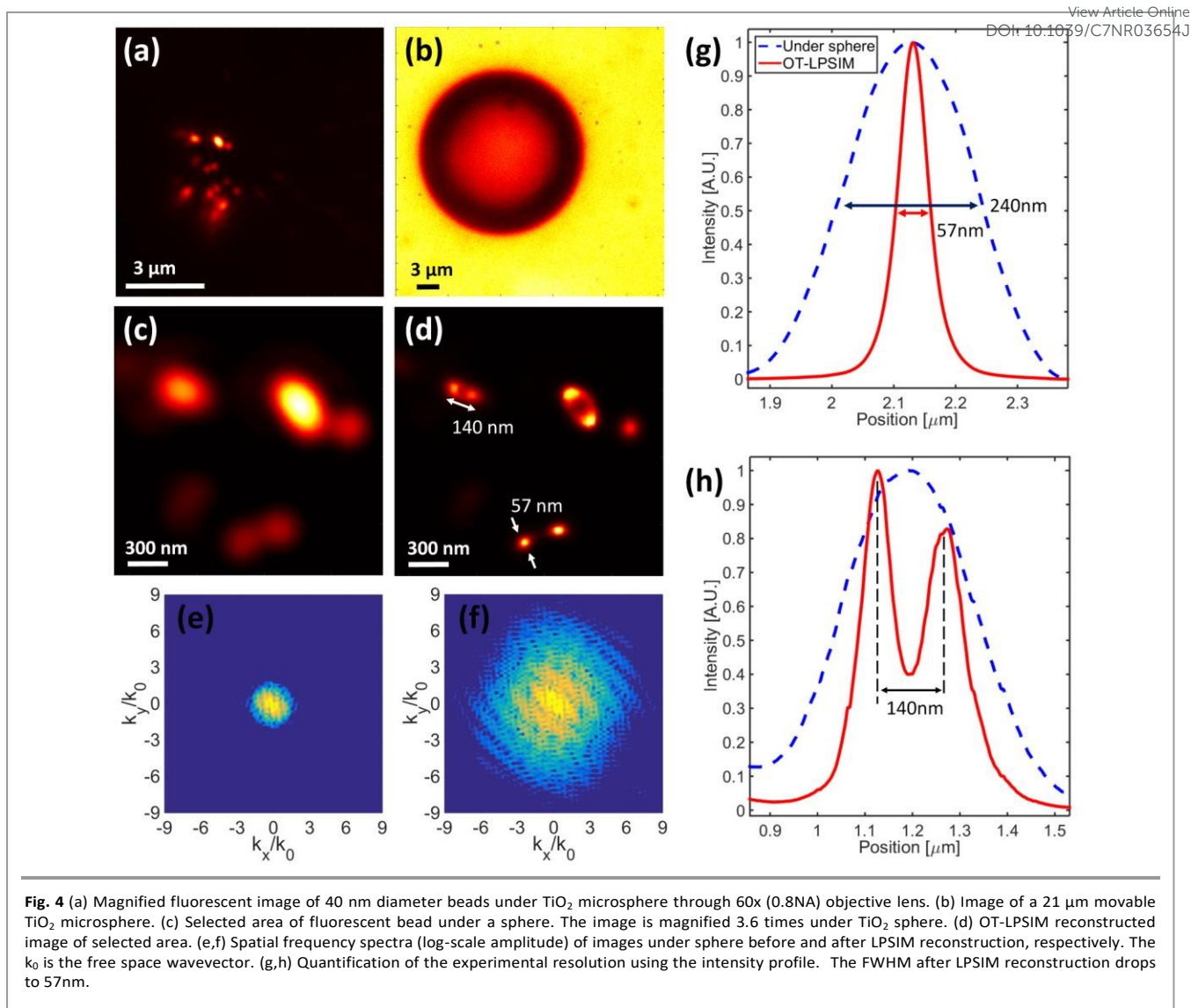
metallic nano-array. The fluorescence was excited by a 488 nm laser and imaged with a 0.8NA 60X air objective.

The resolving capacity of OT-LPSIM was demonstrated by the FWHM of a single-bead at the same location for diffraction-limited image without sphere, under sphere, after LPSIM reconstruction without sphere and under sphere (see Figure 3 d,e,g,h), respectively. Theoretically, an objective with  $NA=0.8$  should have resolution around 435 nm but this objective was used far from its optimized condition in this specific experiment, leading to a lesser resolution to 625 nm. Nevertheless, the effective NA of the system with the microlens was improved to 1.0 according to the Rayleigh criteria  $NA_{eff} = 0.61\lambda/FWHM$ , where  $\lambda$  is emission wavelength and FWHM can be found from experimental data. The polystyrene sphere improved the diffraction limited images of the fluorescence beads by 1.8 times, allowing greater visibility of fine details, and decreased the FWHM from 625 nm down to 350 nm. After applying LPSIM reconstruction

method for regular diffraction-limited image without the microlens, the FWHM decreased more than 3 times, down to 195 nm. For the image under the microlens after LPSIM reconstruction, the final FWHM dropped to 90 nm, representing 7-time resolution enhancement compared to the diffraction limited image obtained from the objective only (Figure 3f). In Figure 3i, it is clearly seen that two closely-spaced beads, which appeared as one bright spot in Figure 3d,e,g, were resolved with OT-LPSIM technique. The center to center distance of the beads was 130 nm, which means edge-to-edge gap between two beads was 90 nm.

#### TiO<sub>2</sub> microspheres

With optically trapped TiO<sub>2</sub> microspheres on top of the LPSIM substrate, we achieved even bigger improvement of resolution. For the experiment, the same 40 nm fluorescent beads were fixed onto a LPSIM substrate with 21  $\mu\text{m}$  TiO<sub>2</sub> microspheres in water on top of it. As the TiO<sub>2</sub> sphere was



moved with the IR optical trapping laser, the area below the microsphere was magnified 3.6 times, as shown in the Figure 4a,b. The effective NA of the system increased to 1.45NA and the diffraction-limited FWHM under sphere decreased from 625 nm to 240 nm.

Significantly, after applying the LPSIM technique, multiple clusters of beads under the TiO<sub>2</sub> microsphere were resolved even farther, allowing distinct separation between neighboring beads, as shown in Figure 4c,d. After LPSIM reconstruction, the FWHM decreased, from 240 nm under microlens, to 57 nm ( $\sim\lambda/10$ ), which provided additional 4.2 times improvement of the TiO<sub>2</sub> microlens (Figure 4g). As a results, if we compare our experimental diffraction-limited FWHM without sphere produced by objective slightly away from its optima position (Figure 3a,f) and the final FWHM with OT-LPSIM using TiO<sub>2</sub> microsphere (Figure 4d,g), the corresponding resolution improvement is  $\sim 11$  times. Figure 4e,f show the corresponding Fourier space spectrum under microsphere with and without the LPSIM technique applied, which confirms the expected

resolution improvement before and after LPSIM reconstruction.

## Conclusions

In this work we demonstrated how the combination of an optically trapped microlens with LPSIM can boost the effective numerical aperture of the imaging system and improve the resolution of existing super-resolution technique. We selected two types of microlens with different size and material: polystyrene microsphere with a relatively smaller index of refraction and TiO<sub>2</sub> microspheres with a higher index, both can be optical trapped and manipulated to desire location. With this new microscopy technique, we achieved 7-11 times improvement of FWHM compared with experimental diffraction-limited FWHM using solely the objective. We believe that the resolution could be easily improved even further by using a long working distance objective, alternative microspheres, shorter operational wavelengths, and more optimal LPSIM substrate. The OT-LPSIM provides a new super

resolution approach that may have great potentials for various imaging applications.

## Acknowledgements

This work was supported by the Gordon and Betty Moore Foundation and the National Science Foundation CBET-1604216.

## Notes and references

‡ Electronic supplementary information includes video files with trapping and moving 46  $\mu\text{m}$  polystyrene sphere and 17  $\mu\text{m}$   $\text{TiO}_2$  sphere with optical tweezers.

- 1 K. I. Willig, B. Harke, R. Medda and S. W. Hell, *Nat. Methods*, 2007, **4**, 915.
- 2 S. W. Hell and J. Wichmann, *Opt. Lett.*, 1994, **19**, 780.
- 3 V. Westphal, S. O. Rizzoli, M. A. Lauterbach, D. Kamin, R. Jahn and S. W. Hell, *Science*, 2008, **320**, 246.
- 4 M. J. Rust, M. Bates and X. Zhuang, *Nat. Methods*, 2006, **3**, 793.
- 5 B. Huang, W. Wang, M. Bates and X. Zhuang, *Science*, 2008, **319**, 810.
- 6 E. Betzig, G. H. Patterson, R. Sougrat, O. W. Lindwasser, S. Olenych, J. S. Bonifacino, M. W. Davidson, J. Lippincott-Schwartz and H. F. Hess, *Science*, 2006, **313**, 1642.
- 7 M. G. L. Gustafsson, *J. Microsc.*, 2000, **198**, 82.
- 8 P. J. Keller, A. D. Schmidt, A. Santella, K. Khairy, Z. Bao, J. Wittbrodt and E. H. K. Stelzer, *Nat. Methods*, 2010, **7**, 637.
- 9 M. G. L. Gustafsson, *Proc. Natl. Acad. Sci. U.S.A.*, 2005, **102**, 13081.
- 10 L. Schermelleh, P. M. Carlton, S. Haase, L. Shao, L. Winoto, P. Kner, B. Burke, M. C. Cardoso, D. A. Agard, M. G. L. Gustafsson, H. Leonhardt and J. W. Sedat, *Science*, 2008, **320**, 1332.
- 11 Y. Blau, D. Shterman, G. Bartal and B. Gjonaj, *Opt. Lett.*, 2016, **41**, 3455.
- 12 D. Li, L. Shao, B. Chen, X. Zhang, M. Zhang, B. Moses, D. E. Milkie, J. R. Beach, J. A. Hammer III, M. Pasham, T. Kirchhausen, M. A. Baird, M. W. Davidson, P. Xu and E. Betzig, *Science*, 2015, **349**(6251), aab3500.
- 13 F. Ströhl and C. F. Kaminski, *Optica*, 2016, **3**, 667.
- 14 F. Wei, D. Lu, H. Shen, J. L. Ponsetto, E. Huang and Z. Liu, *Nano Lett.*, 2014, **14**, 4634.
- 15 F. Wei and Z. Liu, *Nano Lett.*, 2010, **10**, 2531.
- 16 A. I. Fernández-Domínguez, Z. Liu and J. B. Pendry, *ACS Photonics*, 2015, **2**, 341.
- 17 J. L. Ponsetto, F. Wei and Z. Liu, *Nanoscale*, 2014, **6**, 5807.
- 18 J. L. Ponsetto, A. Bezryadina, F. Wei, K. Onishi, H. Shen, E. Huang, L. Ferrari, Q. Ma, Y. Zou and Z. Liu, *ACS Nano*, 2017, **11**, 5344.
- 19 M. G. L. Gustafsson, D. A. Agard and J. W. Sedat, *Proc. SPIE*, 2000, **3919**, 141.
- 20 E. Mudry, K. Belkebir, J. Girard, J. Savatier, E. Le Moal, C. Nicoletti, M. Allain and A. Sentenac, *Nat. Photonics*, 2012, **6**, 312.
- 21 S. M. Mansfield and G. S. Kino, *Appl. Phys. Lett.*, 1990, **57**, 2615.
- 22 A. Darafsheh, N. I. Limberopoulos, J. S. Derov, D. E. Walker Jr. and V. N. Astratov, *Appl Phys Lett.*, 2014, **104**, 061117.
- 23 Z. Wang, W. Guo, L. Li, B. Luk'yanchuk, A. Khan, Z. Liu, Z. Chen and M. Hong, *Nat. Commun.*, 2011, **2**, 218.
- 24 H. Yang, R. Trouillon, G. Huszka and M. A. M. Gijs, *Nano Lett.*, 2016, **16**, 4862.
- 25 P.-Y. Li, Y. Tsao, Y.-J. Liu, Z.-X. Lou, W.-L. Lee, S.-W. Chu and C.-W. Chang, *Opt. Express*, 2016, **24**, 16479. [View Article Online DOI: 10.1039/C7NR03654J](https://doi.org/10.1039/C7NR03654J)
- 26 J. Y. Lee, B. H. Hong, W. Y. Kim, S. K. Min, Y. Kim, M. V. Jouravlev, R. Bose, K. S. Kim, I. C. Hwang, L. J. Kaufman and C. W. Wong, *Nature*, 2009, **460**, 498.
- 27 Y. E. Geints, A. A. Zemlyanov and E. K. Panina, *Opt. Soc. Am. B*, 2012, **29**, 758.
- 28 A. Darafsheh, C. Guardiola, D. Nihalani, D. Lee, J. C. Finlay and A. Carabe, *Proc. SPIE*, 2015, **9337**, 933705.
- 29 L. A. Krivitsky, J. J. Wang, Z. Wang and B. Luk'yanchuk, *Sci. Rep.*, 2013, **3**, 3501.
- 30 E. McLeod and C. B. Arnold, *Nature Nanotech.*, 2008, **3**, 413.
- 31 K. C. Neuman and S. M. Block, *Rev. Sci. Instrum.*, 2004, **75**, 2787.
- 32 A. Ashkin, J. M. Dziedzic, J. E. Bjorkholm and S. Chu, *Opt. Lett.*, 1986, **11**, 288.
- 33 J. Kasim, Y. Ting, Y. Y. Meng, L. J. Ping, A. See, L. L. Jong and S. Z. Xiang, *Opt. Express*, 2008, **16**, 7976.
- 34 T. A. Nieminen, V. L. Y. Loke, A. B. Stilgoe, G. Knöner, A. M. Brańczyk, N. R. Heckenberg and H. Rubinsztein-Dunlop, *J. Opt. A: Pure Appl. Opt.*, 2007, **9**, S196.
- 35 J. E. Molloy and M. J. Padgett, *Contemporary Physics*, 2002, **43**, 241.
- 36 W. H. Wright, G. J. Sonek and M. W. Berns, *Appl. Phys. Lett.*, 1993, **63**, 715.
- 37 K. Dholakia and P. Reece, *Nano today*, 2006, **1**, 18.
- 38 M. Duocastella, F. Tantussi, A. Haddadpour, R. P. Zaccaria, A. Jacassi, G. Veronis, A. Diaspro and F. Angelis, *Sci. Rep.*, 2017, **7**, 3474.
- 39 J. Li, W. Liu, T. Li, I. Rozen, J. Zhao, B. Bahari, B. Kante, and J. Wang, *Nano Lett.*, 2016, **16**, 6604.
- 40 S. P. Gross, *Methods in enzymology*, 2003, **361**, 162.
- 41 A. Darafsheh, *Ann. Phys.*, 2016, **528**, 898.